Fabrication and measurement of optical characterization of one dimensional photonic crystal with defect

Kai Tong (童 凯)*, Fei Wu (吴 飞), and Zhibin Wang (王志斌)

College of Electrical Engineering, Yanshan University, Qinhuangdao 066004, China

**E-mail: tongkai0338@sina.com*

Received January 14, 2009

Numerical calculations based on the transfer matrix method are carried out, and the results of band gap with resonance peaks are obtained. The electron beam lithography technology (EBL) and induction coupling plasma (ICP) etching are used to make the photonic crystal (PC) structures, and from several scanning electron microscope images, the PC structures are observed with features closing to the design. In order to create the tiny PC structures in the right places of the waveguide by the EBL technology at different time, some alignment markers are deposited on the chip, which are made of gold that deposited on titanium for its good adhesion to the underlying Si. An optical testing bed is designed for measurement of the optical characterization of PC structures. Through the analysis of the measured data, a $\Delta\lambda$ value of 0.8 nm is obtained and for the centre frequency of 1547 nm, a very high quality factor value of 1933 can be obtained. The 3-nm difference represents only a 0.2% error from the theoretical centre.

OCIS codes: 220.0220, 260.0260, 310.0310.

doi: 10.3788/COL20100801.0099.

In recent years, the theoretical research, structure design and application technology of photonic crystal (PC) have become a hot research topic in the field of photoelectron[1−3]. It is the major technology for the structure design of PC in the optical signal processing with certain direction or frequency forbidden or transmitted[4,5]. Due to these characteristics, PC has been applied in a wide variety of areas, such as PC lasers[6], filters[7], fibers[8], sensors[9], antennas, laser diodes, and so on.

A very promising application of photonic bandgap (PBG) structures is to improve the performance of waveguides. For example, large enhancement of optical nonlinearity can be achieved more easily by using the high local field of a localized photonic state at a defect in a one dimensional (1D) PC structure. Since local light intensity can be very high at the defect by making use of the localized photonic-defect mode, the optical nonlinearity of the material at the defect can be effectively enhanced by many orders of magnitude[10]. A PC waveguide is basically a PC with a linear defect, which allows the propagation of light in a specific direction[11]. Furthermore, PC waveguides in principle provide a superior guiding mechanism with respect to dielectric or metallic waveguides since their PBG properties make them ideally lossless. Indeed, a straight PC waveguide is actually a system with a discrete periodicity along the waveguide's axis, in which the 1D periodic potential given by the PC may produce mode coupling whenever the Bragg condition is fulfilled. One can easily create a waveguide by removing a row of air holes.

For this purpose, the 1D structure is a highly promising candidate since the incident field is fully coupled to the local mode only in 1D structure. Devices that use this scheme can be fabricated easily by placing thin-film nonlinear optical material in a 1D PC structure. Quarter-wave stacks of two dielectrics with different refractive indices, which have already been used for mirrors or optical filters, are good examples of 1D PC structures. They have a wide PBG centered on the frequency where Bragg reflection takes place. By placing a structural defect at the center of the stack, a photonic-defect state that is localized around the defect can be made.

The PC structure is symmetrical, and the defect layer is sandwiched between two identical stacks of layer of high and low refractive index on a substrate. Each stack is composed of N layers of low refractive indices of the A and B layers, and N layers of high refractive index, B layers. The refractive indices of the A and B layers are denoted as n_A and n_B, and that of the defect layer is n_d. The optical thickness of the A and B layers are d_A and d_B, and that of the defect layer is d_d. They are assumed to satisfy $n_A d_A = n_B d_B = n_\mathrm{d} d_\mathrm{d}/2 = \lambda/2$, where λ is the center wavelength of the incident light. In this case the transmission peak induced by a photonic-defect state appears at the center of the band gap.

The transmission spectrum and local light intensity can be calculated by the method of characteristic matrices. The transmission coefficient of the light field, t, at the midgap frequency with finite absorption of the defect layer, is calculated as

$$t = \frac{-2}{2\cos\left(\frac{\pi k}{n_\mathrm{d}}\right) + \sinh\left(\frac{\pi k}{n_\mathrm{d}}\right)\left[\frac{(n_B/n_A)^{2N}}{1+\mathrm{i}k/n_\mathrm{d}} + \frac{1+\mathrm{i}k/n_\mathrm{d}}{(n_B/n_A)^{2N}}\right]}, \quad (1)$$

where k is the extinction coefficient of the defect layer and is defined as

$$k = \frac{n_\mathrm{d}}{2\pi}\left(\frac{n_A}{n_B}\right)^{2N}. \quad (2)$$

When $k = 0$, the transmittance at the midgap frequency is unity. The transmittance T is

$$T = |t|^2. \quad (3)$$

The spatially averaged intensity of light in the defect layer, supposing that the input intensity is unity, is cal-

1671-7694/2010/010099-04 © 2010 Chinese Optics Letters

culated by

$$G = T\frac{n_{\rm d}}{2\pi k}\sinh\left(\frac{\pi k}{n_{\rm d}}\right)$$
$$\left\{\cosh\left(\frac{\pi k}{n_{\rm d}}\right)\left[\left(\frac{n_B}{n_A}\right)^{2N}\frac{n_{\rm d}^2}{n_{\rm d}^2+k^2}+\left(\frac{n_A}{n_B}\right)^{2N}\right]\right.$$
$$\left.+\sinh\left(\frac{\pi k}{n_{\rm d}}\right)\frac{2n_{\rm d}^2}{n_{\rm d}^2+k^2}\right\}. \quad (4)$$

When $n_B > n_A$, for large N such that

$$(n_B/n_A)^N >> 1, \quad (5)$$

these expressions can be simplified as

$$t = \frac{-2}{2+\frac{\pi k}{n_{\rm d}}\left(\frac{n_B}{n_A}\right)^{2N}}. \quad (6)$$

The intensity enhancement factor, G, at the center defect layer is given by using the transmittance T, as

$$G = \frac{T}{2}\left(\frac{n_B}{n_A}\right)^{2N}, \quad (7)$$

where it is assumed that

$$n_{\rm d} >> k. \quad (8)$$

The dependence of the value of $(n_B/n_A)^{2N}$ can be understood as follows. The local light intensity enhancement at the defect layer is proportional to $(n_B/n_A)^{2N}$, which can be regarded as the effective Q value of the microcavity made by the defect, while in optics, the optical Q factor of a resonant cavity is the ratio of energy stored to energy dissipated in the cavity. The nonlinearity of the raw material, while here nonlinearity means the deviation from linearity in an electronic circuit, an electro-optic device, or a fiber that generates undesired components in a signal, however, should be kept of the order of $(n_B/n_A)^{2N}$ to fully make use of the enhancement. The consequent amount of the change in the extinction coefficient of the order of unity. The effect of this change on transmitted intensity, however, is gained proportional to the intensity enhancement, $(n_B/n_A)^{2N}$. The determination of the number of the PC structure bilayers, N, is important for practical applications. Since the peak width is proportional to $(n_B/n_A)^{2N}$, fluctuation in the layer thickness, or the spectral width of the light utilized, can limit the practical number of layers, which determines the achievable enhancement in the optical nonlinearity.

In order to put the 1D PC structure into a waveguide,

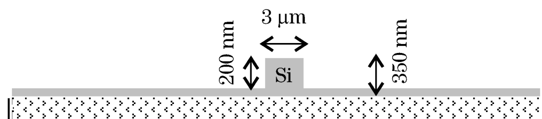

Fig. 1. Side elevation of waveguide based on a Si/SiO2 chip.

which is about 3-μm long and about 200-nm high and created on a Si/SiO_2 chip, an ion milling technology is used during this etching process. As can be seen from Fig. 1, the silicon rib waveguide is designed to be about 3-μm wide and etched about 200-nm depth, for these parameters will guarantee the waveguide to be single mode.

In order to create the tiny PC structures in the right places of the waveguide by the electron beam lithography (EBL) technology, some alignment markers are also required on the chip, and for optimum alignment of the PC structures to the initial waveguides, these markers should be aligned with the waveguides. This marker area is consisted of large number of small squares (both with 16×16 (μm) and 30×30 (μm)), which are made of about 100-nm gold deposited on 50-nm titanium for good adhesion to the underlying Si. Au markers are also used to give a good image during the alignment process under SEM.

The prepared sample was firstly loaded into the EBL chamber, and then several steps including defining mark areas via various operations (e.g., creating position list, filed alignment, write filed corrections, stage adjustment, and finally exposure) were performed stage by stage. After the sample has undergone EBL experiment and resist development, PC patterns were etched into the structure by inductively coupled plasma (ICP), as shown in Fig. 2. This is one of the drying etching methods for creating tiny structures and is chosen for the final etching step on the silicon chip, for that it can result in near vertical side walls, as required to

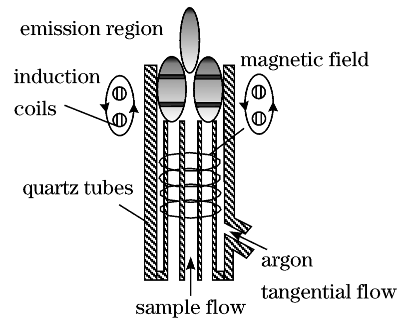

Fig. 2. Schematic of the ICP equipment.

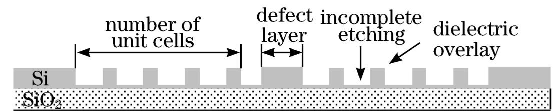

Fig. 3. Schematic side elevation of 1D PC waveguide.

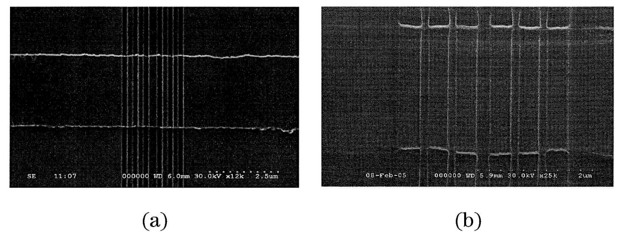

(a) (b)

Fig. 4. SEM image of 1D PC structure of (a) 6 bilayers and (b) 10 bilayers.

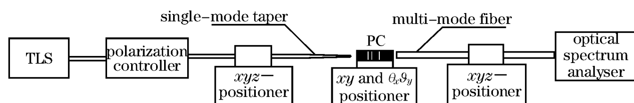

Fig. 5. Schematic of the measurement station.

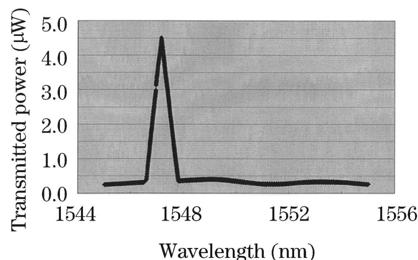

Fig. 6. Fine Measurement of the resonant cavity formed by 0.005-nm wavelength step.

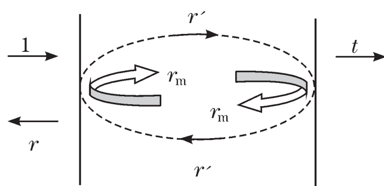

Fig. 7. Minimal mode for recycling radiation in microcavities.

produce accurate structure definition of PC structures. ICP is a very high temperature (7000 - 8000 K) excitation source that efficiently dissociates, vaporizes, excites, and ionizes atoms. Molecular interferences are greatly reduced with this excitation source but not eliminated completely. ICP sources are used to excite atoms for atomic-emission spectroscopy and to ionize atoms for mass spectrometry.

The initial experiment used a 2-min etching time using the plasma and gas flow conditions stated above. The etch depth was assessed using a surface profile machine, from which it was deduced that the etch rate of Si is 55 nm/min and that of polymethyl methacrylate (PMMA) is 70 nm/min. Since the coating thickness of the PMMA is about 200 nm, and the requirement for the depth of the silicon is about 100 nm, PMMA can be used directly for protecting the unetched area. After ICP etching, the final step of the whole fabrication process was to put the chip into acetone solvent again for removing the residual PMMA. The accomplished sample is schematically shown in Fig. 3.

Figure 4 shows two SEM photographs of a completed structure under different magnifications. The device comprises of six 387.5-nm wide air gaps, and four 117.4-nm wide Si sections including a 234.8-nm wide defect layer of Si. As can be seen from the images in Fig. 4, the PC structures are created with high fidelity to the design in the Si waveguides, demonstrating the excellent process control achieved by the EBL and ICP. The good control of the etching produce edges of the PC structures are quite smooth, comparing to the rough sidewalls of the waveguides created by ion milling. To judge whether the modeling and the fabrication results finally create a resonant cavity in the bending waveguide, a butting coupling measurement is given for the accomplished chip.

For the purpose of very fine optical measurement, an optical testing bed, which consists of an air floating bench, an Intun-1500 integrated tunable external cavity laser source, an agilent 11896A polarization controller, a couple of the NanoMax TS 3-Axis Flexure Stages with positioning resolution better than ±10-nm and repeatability, and a specially modified, was fixed on the top of the air floating bench, and it was used for preliminary alignment. Figure 5 shows the setting up of the whole measurement station.

Since the position of the transmission peak is known theoretically, a wavelength region from 1500 to 1560 nm is chosen for very fine data obtaining, and the wavelength step is set to be 0.005 nm. As can be observed from Fig. 6, a resonant peak is observed at 1547 nm, compared with a design wavelength of 1550 nm. The 3-nm difference represents only a 0.2% error, demonstrating the high precision of the fabrication procedure. Further, this result validates the implied design procedure based on the transfer matrix model.

As can be shown from Fig. 6, a resonant transmission peak is detected by the measurement, which means 1D photonic crystal structure works as a resonant cavity filter. The quality factor (Q value), which is normally used to assess the quality of the resonant cavity, is the ratio of energy stored to energy dissipated in the cavity. The Q factor here is defined as the resonant frequency (center frequency) f_0 divided by the bandwidth Δf or bandwidth:

$$Q = \frac{f_0}{f_2 - f_1} = \frac{f_0}{\Delta f} = \frac{\lambda_0}{\Delta \lambda}. \quad (9)$$

Bandwidth $\Delta f = f_1 - f_2$, where f_2 is the upper cutoff frequency and f_1 is the lower one. From Fig. 6, a $\Delta\lambda$ value of 0.8 nm can be obtained and the center frequency is 1547 nm, so the calculated Q value is about 1933. Further, the array of holes in the latter structure includes extra holes designed to improve mode matching between the guided modes of the rib waveguide and the Bloch modes of the PC structure. In theory, the inclusion of such mode matching features will improve the Q value in the Si/SiO_2 1D PC waveguide filters of this letter. For a 1D PC structure with just six bilayers, the reason of such a high Q value can be explained as the so called "radiation recycling". Like classical Fabry-Perot cavities, the model attributes the resonance to a phase-matching of the fundamental waveguide mode along one cavity cycle, but in addition, it encompasses a possible recycling of the radiated field. This recycling is taken into account within the model by introducing a leaky mode in the cavity resonance mechanism, as show in Fig. 7. This representation is reasonable since leaky modes are powerful representations which are often sufficient for describing a portion of the total radiation field in many situations of particular interests.

As shown in Fig. 7, solid and dashed arrows correspond to the fundamental and leaky modes, respectively. Since the cavity is symmetrical, the coupling coefficients r_{m} and r' are the same for both mirrors. Denoting by r' of the reflection-coupling coefficient between the leaky mode and the fundamental mode, one can easily obtain

the master cavity equations as

$$\alpha_1 = t_\mathrm{m} + r_\mathrm{m}\beta_1 + r'\beta_2, \tag{10}$$

$$\alpha_2 = r'\beta_1, \tag{11}$$

$$r = r'_\mathrm{m} + t_\mathrm{m}\beta_1, \tag{12}$$

$$t = t_\mathrm{m}\alpha_1\exp(\mathrm{i}\Phi_1), \tag{13}$$

$$\beta_1\exp(-\mathrm{i}\Phi_1) = r_\mathrm{m}\alpha_1\exp(\mathrm{i}\Phi_1) + r'\alpha_2\exp(\mathrm{i}\Phi_2), \tag{14}$$

$$\beta_2\exp(-\mathrm{i}\Phi_2) = r'\alpha_1\exp(\mathrm{i}\Phi_1), \tag{15}$$

where Φ_1 and Φ_2 are the phase delays through the geometrical cavity length h. $\Phi_1 = k_0 n_\mathrm{eff} h$ and $\Phi_2 = k_0(n' + \mathrm{i}n'')h$ with $n' + \mathrm{i}n''$ being the complex effective index of the leaky mode. α_i and β_i denote the amplitudes of the fundamental and leaky waves traveling to the right and left directions in the cavity. Under the assumption that the mirrors have symmetric refractive index profiles, $r'_\mathrm{m} = r_\mathrm{m}$(reciprocity), Eqs. (10) –(15) are easily solved for the cavity modal transmission coefficient t and reflection coefficient r. Let us denote the effective mirror reflectivity r_eff defined by

$$r_\mathrm{eff} = r_\mathrm{m}[1 + 2(r'/r_\mathrm{m})^2\exp(\mathrm{i}\Phi_2 - \mathrm{i}\Phi_1)]^{1/2}. \tag{16}$$

If we assume that $|r'/r_\mathrm{m}| << 1(i.e., r_\mathrm{eff} \approx r_\mathrm{m} \approx 1)$, an assumption valid for good mirrors, we find

$$t = \frac{t_\mathrm{m}^2\exp(\mathrm{i}\Phi_1)}{1 - r_\mathrm{eff}^2\exp(\mathrm{i}\Phi_2)}, \tag{17}$$

and $r = r_\mathrm{eff}[1 + t\exp(\mathrm{i}\Phi_1)]$. Using the above assumption, the cavity reflection and transmission coefficients can be formally identified as those of a Fabry-Perot cavity whose mirror amplitude mode reflectivity and transmission coefficients are r_eff and t_m, respectively.

Now we could consider an isolated mirror illuminated by the fundamental guided mode with unit light intensity. This guided wave will be partly transmitted with intensity$|r_\mathrm{m}|^2$. Due to the impedance mismatch between the fundamental Bloch mode supported by the mirror and the incident guided wave, a fraction $L = 1 - |r_\mathrm{m}|^2 - |t_\mathrm{m}|^2$ of the energy carried by the incident wave will also be radiated in the air cladding. If we denote by f the fraction of the radiation losses of the isolated mirror which can be potentially recycled inside the cavity by the leaky wave ($f = |r'|^2/L$), then the effective mirror reflectivity of Eq. (16) can be conveniently rewritten as

$$r_\mathrm{eff}/r_\mathrm{m} = 1 + fL/|r|^2\exp(-k_0 n'' h) \times \exp[(\mathrm{i}k_0(n' - n_\mathrm{eff})h + 2\mathrm{i}\theta], \tag{18}$$

where $\theta = \arg(r'/r_\mathrm{m})$. By noting that $|r_\mathrm{eff}|$ is maximum for $\theta = 0$ and $h = 0$, energy conservation for the cavity $(|r_\mathrm{eff}|^2 + |t_\mathrm{m}|^2 < 1)$ imposes an upper boundary for f, namely $f < 0.5$. The effective mirror reflectivity given by Eq. (18) is easily understood. For a cavity length h, the term $fL\exp(-k_0 n'' h)$ in Eq. (18) represents the fraction of the radiated energy recycled by the leaky mode and the argument of last exponential term in Eq. (18) represents the phase shift over one-half cycle of the cavity between the fundamental mode and the recycled leaky mode. Depending on if these modes are phased matched or not, the recycling mechanism can be beneficial or detrimental for the resonator. For good cavities, the correction coefficient in Eq. (18) is small since $|r_\mathrm{m}|^2 = 1$ and $fL\exp(-k_0 n'' h) << 1$. However, because the fundamental mode at resonance bounces many times inside the cavity, weak recycling can take place a great number of times and the cavity T_max, and Q will be significantly increased.

In conclusions, the photolithography and ion milling technologies were used for creating the silicon rib waveguides based on silicon-on-silica insulator, while the waveguides acted as carriers for the PC structures. The EBL and ICP etching were used for making the PC structures, and from several SEM images, the PC structures were observed with features closing to the design. A butt-coupling measurement method was executed for characterizing the fabricated PC structures, while a special testing bed was set up with a computer controlled laser and detector for recording the transmitted power versus wavelength stepping. Through the analysis of the measured data, both the bandgap and resonance peaks were observed, and a very high quality factor value of 1933 was obtained.

This work was supported by the National Natural Science Foundation of China (No. 60877047) and the Specialized Research Fund for the Doctoral Program of Higher Education of China (No. 20070216004).

References

1. Y. Benachour and N. Paraire, Chin. Opt. Lett. **5,** 501 (2007).
2. O. N. Kozina and L. A. Melnikov, J. Non-Cryst. Solids **353,** 968 (2007).
3. E. Galindo-Linares, P. Halevi, and A. S. Sánchez, Solid State Commun. **142,** 67 (2007).
4. W. L. Vos, R. Sprik, A. van Blaaderen, A. Imhof, A. Lagendijk, and G. H. Wegdam, Phys. Rev. B **53,** 16231 (1996).
5. I. I. Tarhan and G. H. Watson, Phys. Rev. Lett. **76,** 315 (1996).
6. T. M. Miller, H. Fang, R. H. Magruder III, and R. A. Weller, Sensors and Actuators A **104,** 162 (2003).
7. S. Gupta, G. Tuttle, M. Sigalas, and K.-M. Ho, Appl. Phys. Lett. **71,** 2412 (1997).
8. A. Ferrando and J. J. Miret, Appl. Phy. Lett. **78,** 3184 (2001).
9. T. Prasad, D. M. Mittleman, and V. L. Colvin, Opt. Mater. **29,** 56 (2006).
10. L. Tang, L. Gao, and J. Fang, Chin. Opt. Lett. **6,** 201 (2008).
11. Z. Li, T. Shen, X. Song, J. Ma, Y. Sheng, and G. Wang, Chin. Opt. Lett. **5,** 696 (2007).